Adsorption of *p*-Cresol by Mesoporous Activated Carbon
II. Mechanism studies and data modeling

MIHAELA NEAGU[1], DANIELA ROXANA POPOVICI[2]*, LOREDANA ELENA VIJAN[3], CATALINA CALIN[2]

[1] Petroleum Gas University of Ploiesti, Department of Petroleum Refining and Environmental Protection Engineering, 39 Bucuresti Blvd., 100680, Ploiesti, Romania

[2] Petroleum Gas University of Ploiesti, Department of Chemistry, 39 Bucuresti Blvd., 100680, Ploiesti, Romania

[3] University of Pitesti, Department of Natural Sciences, 1 Targu din Vale Str., 110040, Pitesti, Romania

In this work, the adsorption mechanism of p-cresol from aqueous solution onto mesoporous activated carbon was investigated. The mechanism of the adsorption process was determined from Weber-Morris and Boyd models. By graphical and statistical analysis was demonstrated that both film-diffusion and intra-particle diffusion are concurrent in adsorption mechanism. The adsorption mechanism of p-cresol onto mesoporous activated carbon was sustained by FTIR analysis, Boehm titration and the point of zero charge of the GAC.

Keywords: adsorption; mechanism; activated carbon; p-cresol

Organic compounds are common pollutants of wastewaters derived from many industries such as pesticides industries, dyes, tanning, textile, plastic, rubber, paper and pulp manufacturing, petrochemical and petroleum refineries [1-3]. Cresols are very toxic to human and animal life and resistant to biodegradation. Therefore, it is essential to remove them before discharge into the environment. Among the various treatment methods, adsorption is currently being used extensively for the removal of organic compound from water.

The aim of this study is to investigate the adsorption mechanism of *p*-cresol onto mesoporous activated carbon. The mechanism of the adsorption process was determined from Weber-Morris and Boyd models. In order to assess the parameters of the models, the linear regresion was applied and an statistical analysis was conducted. The statistical analysis takes into account the sum of the squares of the errors *SSE,* the coefficient of determination R^2, the adjusted coefficient of determination *Adj* R^2 and the standard deviation *SD* values to check the accuracy of fit measure. FTIR analysis, Boehm titration and the point of zero charge of the GAC were used to explain the adsorption mechanism.

Experimental part
Materials and methods

The main materials used in this work were the granular activated carbon (GAC) and *p*-cresol. In the first part of our research [4], it was presented the procedure whereby the experimental kinetic data were obtained. The physical charaterisation of GAC has been reported in previous studies [5-7]. The surface of the GAC was chemically characterized by Boehm titration [8] and by point of zero charge pH_{PZC} [9], and the results were reported in our previous study [5].

Fourier Transform Infrared (FT-IR) spectra were recorded with a Bruker Spectrometer FT-IR Tensor 27 to qualitatively characterize surface groups on activated carbon used in this study. FT-IR spectra were recorded in KBr pellets.

Adsorption mechanism modeling

Nowadays, the intra-particle diffusion model of Weber-Morris and the film-diffusion model of Boyd are the two most widely used models for studying the mechanism of adsorption [10,11]. The equations of Weber-Morris and the Boyd models are presented in table 1.

Weber-Morris model assume that the adsorption process is intra-particle diffusion controlled if the rate is dependent upon the rate at which adsorbate diffuse into adsorbent [12]. It can be seen from eq. (1) that the intra-particle diffusion would be the only controlling step in the adsorption process if the plot of the amount of the adsorbent per unit mass of adsorbent (q_t) against square root of time ($t^{0.5}$) is a straight line with a slope that equals k_{id} and this line passed through the origin [13].

Boyd model is a film-diffusion that assumes that the main resistance to diffusion is in the film surrounding the adsorbent particle [14,15]. El-Khaiary and Malash [17] recomended to use both eqs. (4a) and (4b) in order to avoid the distortion of Boyd model. The intraparticle-diffusion controls the rate of mass transfer if the *Bt* versus time is linear and passes through the origin then. If the plot is linear or nonlinear but does not pass through the origin, then the film diffusion or chemical reaction controls the rate [18].

Results and discussions
FTIR spectra of the granular activated carbon

The FT-IR spectra was used to examine the surface groups of GAC and to identify the groups participating in *p*-cresol adsorption (fig. 1).

The spectra of GAC show a band at 2328 cm^{-1} that can be assigned to the ammonium salts (2250 – 2700 cm^{-1}), corresponding to the N-H stretching vibration. The presence of the aliphatic tertiary amines it is confirmed by 1034 cm^{-1} band, characteristic to C – N stretching vibration (1020 – 1230 cm^{-1}). The band at 1566 cm^{-1} can be assigned to the characteristic out-of-phase stretching vibration of $–COO^-$ from carboxylic acid salts [19]. The shoulder at about 1250 cm^{-1} was attributed to the C – O stretching vibration from the phenols (1180 – 1260 cm^{-1}) [19]. The bands from the range 600 – 900 cm^{-1} can be assigned to the out-of-plane bending vibration of the C – O or C – H group [20].

Although the acidic functional groups predominate, the surface of granular active carbon also contains the basic

* *email: dana_p@upg-ploiesti.ro; Phone: (+40)722295989*

Models	Equation	Eq. no.	Parameters	Ref.
Weber-Morris	$q_t = k_{id} t^{0.5} + C$	(1)	k_{id} (mg g^{-1} min $^{0.5}$) is the intra-particle diffusion parameter C (mg g^{-1}) is the intercept which represents the value of the thickness of the boundary layer	[12]
Boyd	$F(t) = 1 - \left(\frac{6}{\pi^2}\right)\sum_{n=1}^{\infty}\left(\frac{1}{n^2}\right)\exp\left(-n^2 Bt\right)$ $F = \frac{q_t}{q_e}$ For $F(t)$ values > 0.85, $Bt = -0.4977 - \ln(1 - F(t))$ For $F(t)$ values < 0.85, $Bt = \left[\sqrt{\pi} - \sqrt{\pi - \left(\frac{\pi^2 F(t)}{3}\right)}\right]^2$	(2) (3) (4a) 4(b)	$F(t)$ is the fractional attainment of equilibrium, at different times t, Bt is a constant, (min^{-1})	[16]

Table 1
WEBER-MORRIS AND THE BOYD MODELS

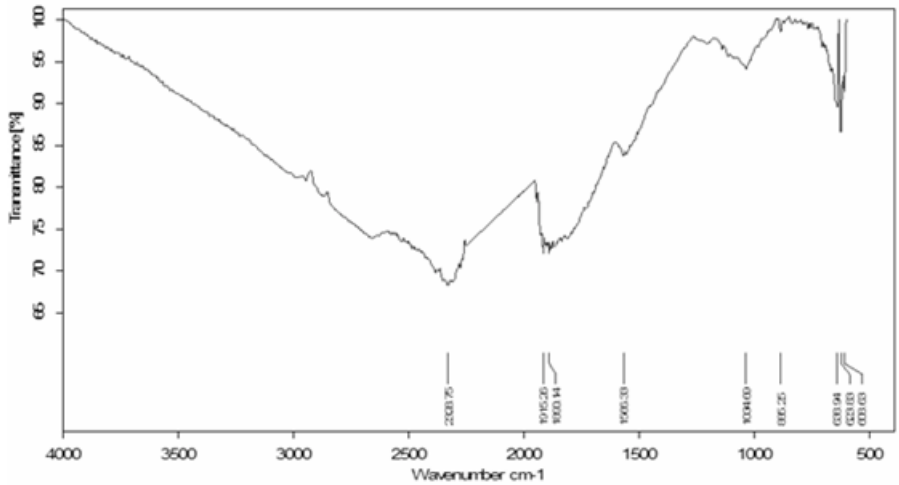

Fig. 1. Infrared spectra of activated carbon

functional groups [5]. Even if quantitative the acidic groups are three times more than basic groups, the last ones seem to be stronger given the almost neutral point of zero charge (pH_{PZC}). In this respect, it can be assumed that the basic groups could be mainly the tertiary amines identified by FTIR spectroscopy.

Adsorption mechanism

The adsorption mechanism were analyzed by the intra-particle diffusion model of Weber-Morris and the film-diffusion model of Boyd to elucidate the diffusion mechanism in the adsorption of *p*-cresol onto the GAC adsorbent.

Figure 2 shows the adsorption profiles by plotting q_t versus $t^{0.5}$ for three initial concentration of *p*-cresol on GAC. By analyzing the data in figure 2, two or three linear segments are depicted, according to *p*-cresol initial concentrations. At 1000 mg L^{-1} *p*-cresol concentration in feed solution, the plot q_t versus $t^{0.5}$ indicates that intra-particle diffusion was not the only process involved in solute adsorption, and there coexist an other process which may be involved in the rate controlling step [21,22]. In the firsts

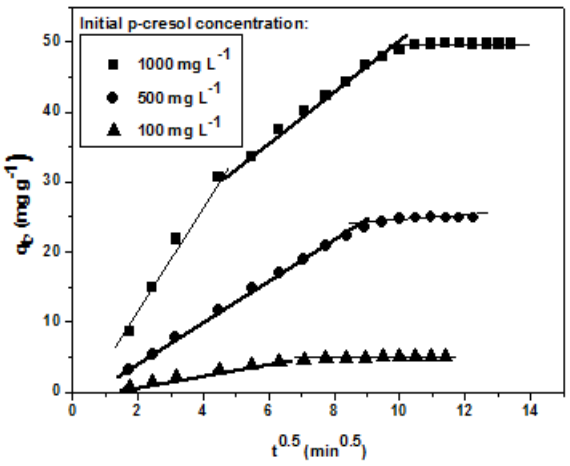

Fig. 2. Intra-particle diffusion plots for the adsorption of *p*-cresol onto GAC for different initial feed concentrations

20 min occurs the very fast transport of adsorbate molecules due to the greater concentration driving force from bulk solution to the external surface of adsorbent and than the adsorption step slows down when the external transport (diffusion) through the boundary layer of *p*-cresol start-up. The second stage (bold line in fig. 2) shows the gradual adsorption from 20 to 90 min, where the adsorbate is transferred to the interior of the particle by diffusion of *p*-cresol molecules through macropores, mesopores and micropores [22]. In this stage, the intra-particle diffusion was the rate limiting step [23]. Finally, the third step shows the formation of plateau which indicate the equilibrium stage and maximum adsorption [21]. On the other hand, at 500 and 100 mg L^{-1} *p*-cresol concentration in feed solution, the plots q_t versus $t^{0.5}$ show only two stage. The first stages (bold line in fig. 2) can be explained as gradual adsorption where intra-particle diffusion can be one of the rate limiting step. In other words, these first stages do not exclude the involvement of the film diffusion in adsorption rate controlling. The second stages it is described as equilibrium stages where intra-particle diffusion becomes limited due to the depletion of the solution *p*-cresol.

Figure 2 also ilustrate that the plots did not pass through the origin, and consequently the intercepts *C* is different of zero. This further support the idea that the intra-particle diffusion is involved in the adsorption process, but is not the only rate-controlling step. The rate parameter k_{id} corresponding to the intra-particle diffusion stages and the intercept *C* values are reported in table 2 together with the error function values.

Table 2
PARAMETERS OF WEBER-MORRIS MODEL AND ERROR FUNCTIONS VALUES

C_0 (mg L^{-1})	100	500	1000
k_{id} (mg g^{-1} $min^{0.5}$)	0.78130	2.84911	3.52362
C (mg g^{-1})	-0.50042	-1.18084	14.8378
SSE	0.07314	0.38148	1.52352
R^2	0.99258	0.99777	0.99694
Adj-R^2	0.99073	0.99745	0.99643
SD	0.13522	0.23345	0.50390

By analyzing the data listed in table 2, it can be seen that the error function values (i.e. high correlation coefficients R^2 and *Adj-*R^2 values and low values of *SSE* and *SD*) support the choice of the linear segments from *qt* versus $t^{0.5}$ graph in order to finding the parameters of the intra-particle diffusion model. The values of k_{id} was found to increase with the initial *p*-cresol concentration increasing. The intercept values suggests that the film diffusion can be involved in adsorption mechanism. In order to support these considerations, the experimental data were analysed by Boyd model. The Boyd model is frequently applied to kinetic data to analyse whether the rate limiting step is intra-particle diffusion or film diffusion. The plots *Bt* versus *t* were obtained with data calculated from both eqs. (4a) and (4b) based on experimental value of *qe*. Figure 3a shown the plots *Bt* versus *t* over the entire time period and over the studied range of p-cresol initial concentrations. From the extended graph, it can be observed that the plots are non-linear, do not passes through the origin and shows one or two linear segments at the beginning of the adsorption (fig. 3). Nowaday, only few researchers deals with these segments by the graphical and statistical analysis in order to support their conclusions [22,24]. The embedded graph in figure 3b show few segments to the film-diffusion model for the experimental data that were fitted linear. The values of intercepts together with their error function values are listed in table 3. It is observed low values of *SSE* and *SD*, and also the high value of correlation coefficients R^2 and *Adj-*R^2 which is a strong evidence that support our decision in the selection of the linear segments for the experimental data examination by Boyd model.

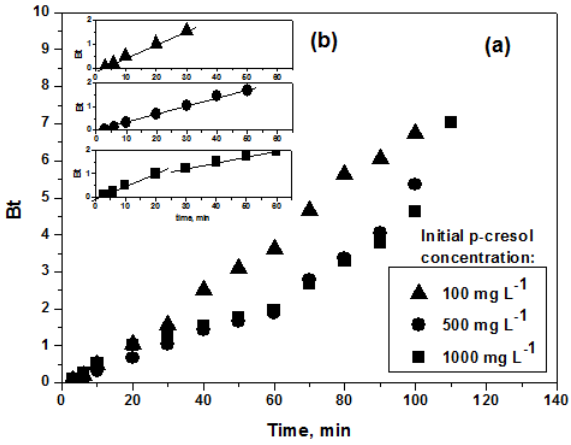

Fig. 3. Boyd plots for the adsorption of *p*-cresol onto GAC for different initial feed concentrations

The adsorption mechanism of *p*-cresol on activated carbon is dependent to a large extent on the chemistry of carbon surface. The heterogeneous surface of activated carbon was confirmed by FT-IR and Boehm titration as was presented previously. According to Kennedy et al. [25] and Neagu and Vîjan [6] the physical adsorption of *p*-cresol as of the other aromatic compounds onto activated carbon occurs probably through dispersive interactions between the aromatic rings and the carbon planes (π–π interactions), on the one hand, and surface groups (especially oxygen containing groups), on the other hand. The *p*-cresol molecules appers to be orientated predominantly in vertical position on the plan of the carbon

C_0 (mg L^{-1})	Segments	Intercept	*SSE*	R^2	*Adj-*R^2	*SD*
100	First segment	-0.10195	0.00399	0.99745	0.99660	0.03645
500	First segment	-0.05633	0.00939	0.99622	0.99546	0.04333
1000	First segment	-0.07131	0.00211	0.99583	0.99375	0.03250
	Second segment	0.16183	2.40×10^{-4}	0.98071	0.96142	0.01548

Table 3
PARAMETERS OF BOYD MODEL AND ERROR FUNCTIONS VALUES

surface. In our previously work [6] it has been demostrated that *p*-cresol exhibits electron donating mechanism with the carbonyl and basic active sites. On the surface of GAC the basic sites could be represented by tertiary amines (identified by FT-IR spectra but also by Boehm titration [5]) and the carbonyl sites could by associated with lactonic groups highlighted by Boehm titration [5].

Considering foregoing discussions, the posible mechanism of *p*-cresol adsorption occurs on boundary layer around to carbon surface and its magnitude depends by adsorbate concentration in bulk solution. In the intra-particle step, the micropore filling mechanism of the smallest micropores is in competition with the adsorption on surface active centers located in larger micropores or in mesopores [26]. The presence of mesopore in activated carbon studied in this work has two beneficial roles: enable the rapid access of *p*-cresol molecules from the bulk solution to the deeper micropores without any impediment and also increase the equilibrium coverage of micropore surface [26].

Conclusions

Intra-particle diffusion model and film-diffusion model has been applied to identify the adsorption mechanism. Both plots shows multi-linearity and all relevant segments were tested by the graphical and statistical analysis. The results indicate that the film-diffusion and intra-particle diffusion are concurrent in overall rate adsorption control. The heterogeneous surface of activated carbon was confirmed by FT-IR spectra and Boehm titration. The physical adsorption of *p*-cresol onto activated carbon occurs probably mainly through π–π interactions and electron donating mechanism.

Acknowledgment: The authors gratefully acknowledge PhD Emilia Oprescu for their assistance at the recording of the FT-IR spectrum for the granular activated carbon.

References

1. CAETANO M., VALDERRAMA C., FARRAN A., CORTINA J.L., Journal of Colloid and Interface Science, **33**, 2009, p. 402 409;
2. KUMAR A., KUMAR S., KUMAR S., GUPTA D.V., Journal of Hazardous Materials, **147**, 2007, p. 155-166;
3. SADHUKHAN S., SINGHA S., SARKAR U., Chemical Engineering Journal, **152**, 2009, p.361-366;
4. NEAGU, M., POPOVICI, D.,DUSESCU, C.M., CALIN, C., Rev. Chim. (Bucharest), **68,** no. 1, 2016, p. 139
5. NEAGU M., POPOVICI D., Rev. Chim. (Bucharest), **66**, no. 7, 2015, p.1004
6. NEAGU M., VIJAN L.E., Environmental Engineering and Management Journal, **10,** 2011, p. 181-186;
7. VIJAN L.E., NEAGU M., Revue Roumaine de Chimie, **57**(2), 2012, p. 85–93;
8. BOEHM, H.: Adsorption by carbons. Chapter- Surface chemical characterization of carbons from adsorption studies, Elsevier, Bottani E.J., Tascon J.M.D. (eds), Amsterdam, 2008, p. 301-327;
9. RODRIGUES L.A., DA SILVA M.L.C.P., ALVAREZ-MENDEZ M.O., DOS REIS COUTINHO A., THIM G.P., Chemical Engineering Journal, **174**, 2011, p. 49-57;
10 AHMAD R., KUMAR R., LASKAR M.A., Environmental Science and Pollution Research, **20**, 2013, p. 219-226;
11. NATH K., PANCHANI S., BHAKHAR M.S., CHATROLA S., Environmental Science and Pollution Research, **20**, 2013, p. 4030-4045;
12. WEBER W.J., MORRIS J.C., Journal of Sanitary Engineering Division, **89**, 1963, p. 31-60
13. WU Z., ZHONG H., YUAN X., WANG H., WANG L., CHEN X., ZENG G., WU Y., Water Research, **67**, 2014, p. 330-344;
14. DOLININA E.S.; PARFENYUK E.V., Journal of Solid State Chemistry, **209**, 2014, p. 105–112;
15. KAVAK D. D., ULKU S., Process Biochemistry, 50(2), 2015, p. 221–229;
16. BOYD G.E., ADAMSON A.W, MYERS-JR L., Journal of American Chemical Society, **69**, 1947, p.2836–2848;
17. EL-KHAIARY M.I. MALASH G., Hydrometallurgy, **105**, 2011, p. 314–320;
18. HAMEED B.H., EL-KHAIARY M.I., Journal of Hazardous Materials, **159**, 2008, p.574–579;
19. LARKIN P., IR and Raman Spectroscopy. Principles and Spectral Interpretation, 1st Edition, Elsevier, Amsterdam, 2011, p. 73-115;
20. LIU Q.S., ZHENG T., WANG P., GUO L., Industrial Crops and Products, **31**, 2010, p.233–238;
21. REN Y., ABBOOD H.A., H.E F. PENG H., HUANG K., Chemical Engineering Journal, **226**, 2013, p.300–311;
22. HOSSEINI S., KHAN M. A., MALEKBALA M. R., CHEAH W., CHOONG T., Chemical Engineering Journal, **171**, 2011, p.1124–1131;
23. TEOH Y. P., KHAN M. A., CHOONG T., Chemical Engineering Journal, **217**, 2013, p.248–255;
24. MALASH G., EL-KHAIARY M.I., Chemical Engineering Journal, **163**, 2010, p.256–263;
25. KENNEDY L.J., VIJAYA J.J., SEKARAN G., KAYALVIZHI K., Journal of Hazardous Materials, **149**, 2007, p.134–143;
26. TERZYK A.P., Journal of Colloid and Interface Science, **268,** 2003**,** p.301–329

Manuscript received: 28.03.2016